Research paper

Proposal of concept for global analysis of hybrid beams – numerical investigation

Maciej Kożuch[1], Łukasz Skrętkowicz[2]

Abstract: Investigation on the behaviour of hybrid beams is presented. Hybrid beam stands for an element with hybrid cross sections. This means sections that consist of steel and concrete parts, connected together with composite dowels, and both are considered for shear flow analysis. In practice, a more general solution may be used for bridges in the form of a beam in which the span sections are hybrid and the support sections are concrete. For the first time in the world, it was decided to introduce a girder in bridge construction, in which a concrete web with a thickness of only 20 cm was formed, directly connected to the steel web, so that a hybrid cross-section is created in accordance with the new European design regulations currently being developed (1994-1-102). The solution is new itself and requires also a new approach for internal forces determination. In this paper a parametric analysis of different hybrid beams with span range from 20 to 40 m and with different reinforcment ratio is performed to get knowledge on the influence of (1) concrete cracking and (2) rheology of concrete on the redistribution of internal forces. Results are analysed and conclusions are presented. As a final step, a general method for computer aided modelling of hybrid beams (*hybrid beam concept*) is proposed, which is based on the uncracked analysis. Such an analysis is designer-friendly and while appropriate benchmarked (as in this paper) can spare a lot of time needed for detailed iterative cracked analysis.

Keywords: composite bridge, hybrid beam, tension-stiffening effect, composite dowels shear connection

---

[1]PhD. Eng., Wroclaw University of Science and Technology, Faculty of Civil Engineering, Wybrzeże Wyspiańskiego 27, 50-370 Wrocław, Poland, e-mail: maciej.kozuch@pwr.edu.pl, ORCID: 0000-0002-1743-5233
[2]MSc. Eng., Wroclaw University of Science and Technology, Faculty of Civil Engineering, Wybrzeże Wyspiańskiego 27, 50-370 Wrocław, Poland, e-mail: lukasz.skretkowicz@pwr.edu.pl, ORCID: 0000-0001-5174-1798

1. Introduction

Currently, a large research program is being completed by Wrocław University of Technology (together with industrial partners), which includes the analysis of hybrid steel-concrete beams (Fig. 1), the aim of which is to implement a new type of hybrid beams with the smallest possible concrete web thickness in bridge construction (this is an utilitarian goal imposed by industrial partners, while two scientific goals are pursued at the same time: confirmation of the concept of a hybrid cross-section with full-scale tests and development of a global analysis method). The article deals with the second issue and the background of events is presented below so that the reader fully understands why certain scientific issues were solved in this and not another order.
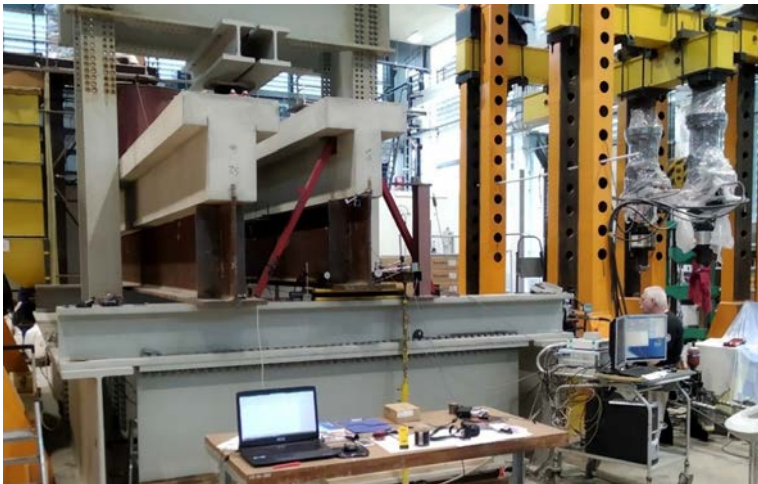

Fig. 1. Hybrid beams prepared for tests in lab

Bridges using composites dowels have been built in Poland and the EU for over 10 years [1] and the European design rules CEN/TS 1994-1-102 is currently being proposed, introducing the rules for designing both the shear connection and new types of cross-section; so called hybrid section. The first bridge designed in accordance with the hybrid section concept proposed in CEN is the structure presented in [2]. Publication [2] highlights the problems related to global analysis, which have been discussed all the time and so far no consensus has been reached on how global analysis of such objects should be carried out. At this point, it is noted that solutions such as those presented in [3] are still perceived as innovative and designed by a small group of engineers with appropriate knowledge – they are niche solutions. Development of a new form of composite dowel shear connection in 2019, the so-called SRCD [4] enabled a significant reduction in the thickness of the concrete web (Fig. 1: beam on the right side) and was a step towards construction of hybrid beams for road bridges with characteristics that would allow them to compete on the market with prestressed concrete precast elements. It is the concept of developing the

entire system of typical road bridges with hybrid beams used in continuous systems that has resulted in comprehensively addressing the issue of how to perform the global analysis, and in particular the new problem of redistribution of bending moments in hybrid beams [3]. Bridges created in the new system are currently being built in Poland (Fig. 2 and 3).
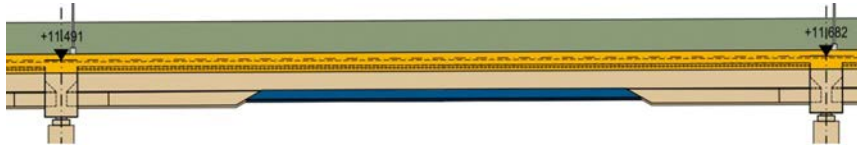

Fig. 2. Typical span of one of multi-span L = 36 m continuous hybrid bridge of S3 express way [5]
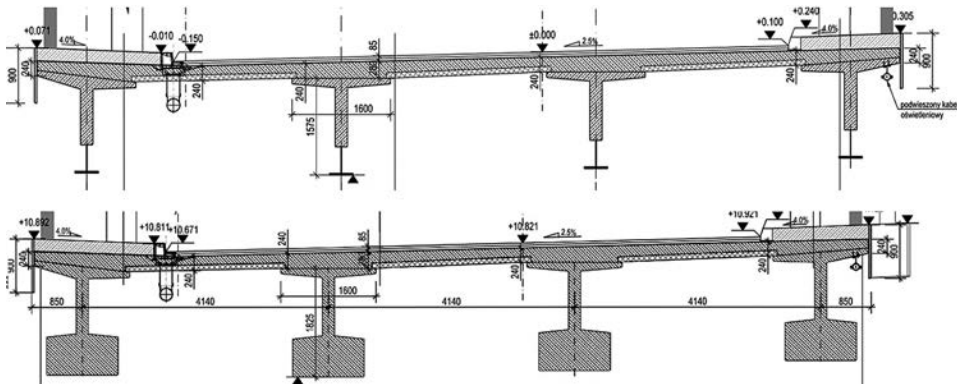

Fig. 3. Typical mid-span and internal support cross-sections of one of multi-span continuous hybrid bridge of S3 express way [5]

And at the same time individual solutions are being developed where the new concept of determining internal forces is also used. The method proposed for the global analysis should be just as universal as possible and enable the analysis of various solutions with hybrid cross-sections (not only those shown in Fig. 2 and 3). For example, Figs. 4 and 5 show a new bridge designed by the authors and currently being built in a different system [6, 7] used for the continuous spans of about 50 m. This solution uses classic composite sections in the spans and new hybrid sections (double composite action) above the piers. In the course of the project, independent "cracked" an "un-cracked" global analysis have been done and conclusions were drawn in support of the theses presented in this article. In particular (and not for the first time – similar conclusions were made in [2]) it was noted that the analysis in the un-cracked state of the support zones allows for easier modeling and design of the bridge slab in the complex stress state in the support zone.

It should be noted that in the past, Eurocode 4 clauses were created for modeling only with beam elements and their use in the case of shell models raises difficulties when one wants to apply cracked concrete in the longitudinal direction and properly include the slab for local loads and effects (in particular, currently most bridge models are made
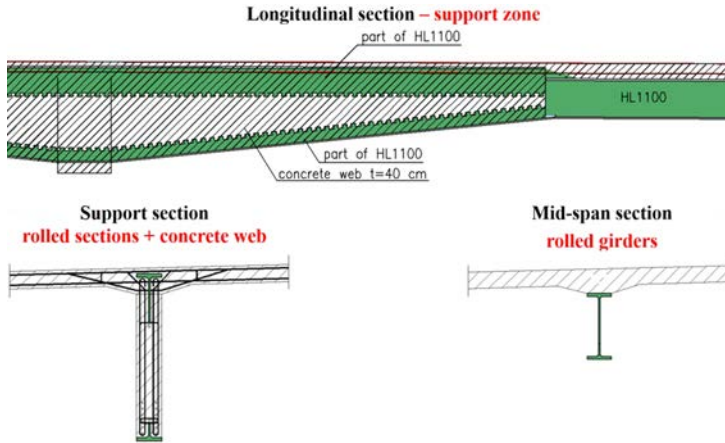
Fig. 4. General idea of the support zone of a new hybrid bridge designed by authors [6, 7], so called *Crocodile* solution (top and bottom T-beams with composite dowels create a shape of crocodile jaws)
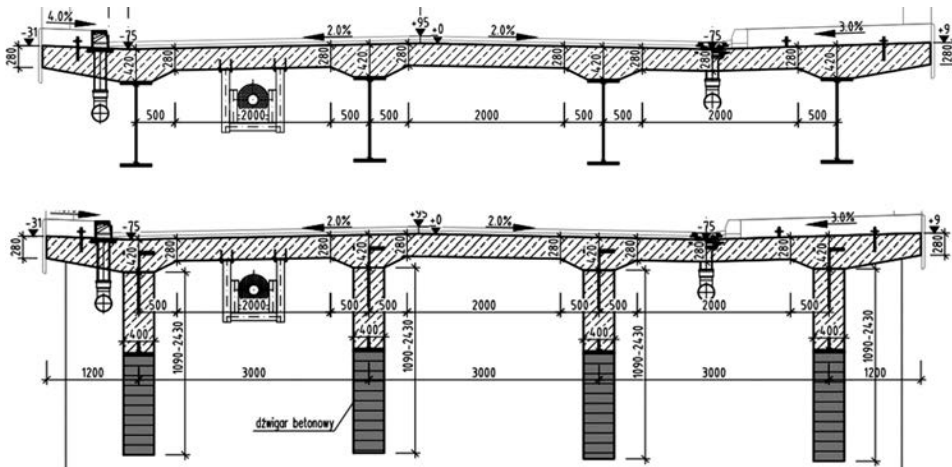

Fig. 5. Typical mid-span and internal support cross-sections of the *Crocodile* hybrid bridge

with such a plate model; see Fig. 6). A classic example of such a problem is an arch bridge with a tie in the form of a concrete slab connected to a steel girders (composite deck) and not prestressed – cracking of the slab (in the model) may significantly disturb the distribution of bending moments in the slab which is supported on crossbeams and longitudinal beams [8]. The question of whether concrete cracking should relate to axial stiffness only or to both axial stiffness and flexural stiffness of the slab is a frequently discussed issue. Fig. 6 shows the model used in analysis of the bridge presented in Figs. 4 and 5: for the purposes of reinforcement design, a model with an uncracked concrete slab was adopted and the mapping is sufficient to adequately account for both global and

local effects. The above considerations were quoted in order to justify why the authors propose to change the currently used methods of modeling girders due to cracking. This is related to the experience they have gained modeling many new type (hybrid) structures and encountering problems that need to be solved.
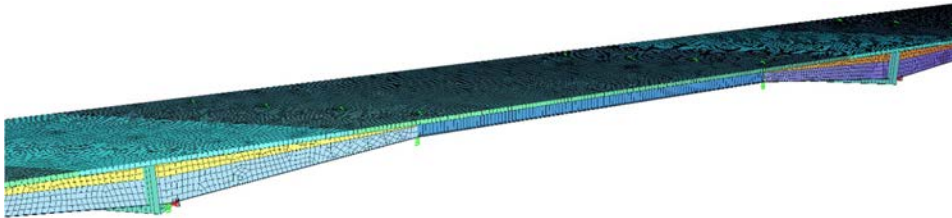

Fig. 6. Shell model of a hybrid bridge, on example of the *Crocodile* bridge presented in Figs. 4 and 5

In a paper [3] a brief overview of composite dowels development [9–11] and existing and recently designed hybrid-beam type constructions was presented, and some motivators – mostly economical – for their development were described. Hybrid beams, comparing to standard steel-concrete composite structures, offer significantly less structural steel consumption [1, 6, 12–15], and (depending on the market trends) this is usually the most decisive aspect of economical success of a design. However, design of hybrid beams goes beyond rules and requirements established in the current standards. Two key aspects were distinguished as crucial for structural analysis. The first one is the issue of shear force flow (discussed in [16-19]), the second one is the issue of the redistribution of bending moments due to concrete cracking and its rheology, and how to handle it during design without utilization of advanced methods, difficult to apply during everyday design, mentioned in [3, 20]. The issue of shear force transfer in such a cross section has already been described, and the dimensioning procedure is known at the level of cross section (*hybrid cross section concept*) [16–19, 21]. The so called *hybrid beam concept* (describing problem of the second aspect – bending moment redistribution due to concrete cracking and its rheology) is now under consideration.

Just to give a short overview on the discussion conducted in [3] a Fig. 7 is hereafter presented. It shows differences in terms of cracking between reinforced concrete (RC), steel-concrete composite and hybrid beams. One can notice that cracking zones are different in all 3 solutions. For RC beams undergo cracking in both mid-span and intermediate support zones, thus there is no significant bending moments redistribution due to cracking (and similarly due to rheology). For standard composite beams with concrete plate on top of steel section, cracking occurs only in a slab in hogging bending moment's zones – procedure for concrete cracking accounting in a design are precisely described in relevant standards (e.g. [22,23]). Contrary to above mentioned situations, for hybrid beams cracking of concrete occurs due to both sagging and hogging moments, but in mid-span sections only in a range of tensile concrete web. Design procedures allowing to handle phenomenon of concrete cracking and its influence on global bending moments redistribution do not exist. Moreover, exact determination of cracked zones, requires in this case an iterative

procedure, because decrease in stiffness in one region causes a change not only in bending moment diagram, but also redistribution on stresses within one considered cross section (for example – cracking of concrete slab will cause developement in cracked zone also toward concrete web).
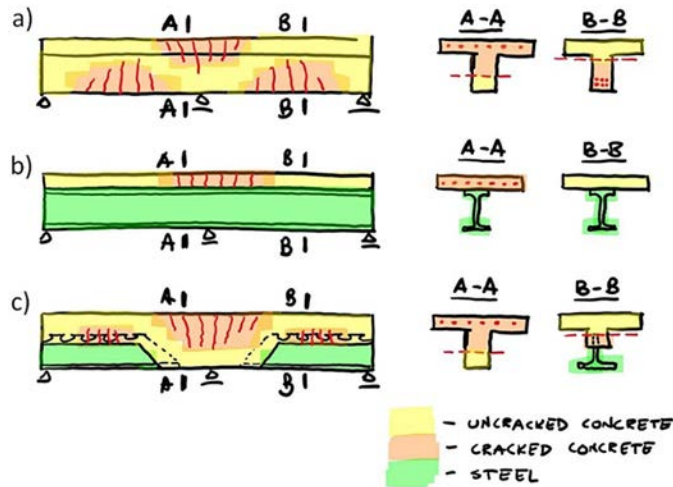

Fig. 7. Concrete cracking ranges in (a) reinforced concrete beam, (b) composite beam, (c) hybrid beam [3]

Layout for hybrid beams modelling technique in abovementioned aspect was given in the paper [3]. It was discussed how the way of modelling of cracking of concrete and its rheology influences global bending moments envelopes. 4 different approaches were considered: uncracked analysis and 3 approaches enabling for concrete cracking: two of them as modified appraches based on EC4 [23] recommendations and one taking into account full stress-strain paths for concrete parts basing on the known reinforcement ratios. Performed analysis prooved that concrete cracking may significantly change bending moments in the hybrid beam, while rheology influence is of minor importance (in opposite to standard steel-concrete composite beams). Moreover, regardless of the way of concrete cracking modelling, the final results were nearly the same. This conclusion lays the foundations for using one of the methods for furhter parameric studies. As a proposed design concept of the hybrid beam (for further considerations) it was stated to make a complete reversal of the concept used as standard in EC4 for the needs of the hybrid beam global analysis: uncracked analysis with bending moment redistribution. This redistribution would be a decreasing of hogging moments for example of 5% and increasing the sagging ones of up to 15%. These particular limits were suggested safe-sided on basis of 1 considered example, covering all deployed design approaches. The aim of this paper is to verify conclusions presented in the first part [3] and to justify or modify the proposed redistribution limits on basis of performed additional bigger-scale analysis covering FE-analysis of hybrid beams with span range from 20 to 40 m and with different reinforcement ratio.

2. Finite element analysis

In this section, numerical analysis is carried out to show how the concrete cracked zones develop in a hybrid beam and how this phenomenon affects the bending moments' distribution along the beam. Influence of creep and shrinkage of concrete is also under investigation. Analysis is conducted for five different span lengths, chosen this way to cover expected spans range for hybrid beams application.

2.1. Numerical analysis

In the paper [3], the exemplary girder from a newly designed bridge on S3 road [5] had been analysed. Based on that girder geometry some enhancement and adaptation were made to make a parametric analysis of large variety of possible beams' geometries.

Parametrised geometry of analysed girders is shown in Fig. 8. For the purpose of analysis, it is assumed that *in-situ* concrete slab (concrete C30/37), with a thickness of 24 cm, is casted with fully propped precast girder (which is made out of S460N steel and C50/60 concrete). Thus, after removing the temporary supports, it is subjected to participate in the actions taken from its self-weight too. Longitudinal reinforcement in hogging moments zone is in:

- *in-situ* slab: parametrised by rebar spacing r_1 and r_2 and its diameter. Detailed description is in the next paragraph.
- upper slab of precast element: arranged in one layer, #20/150 (what means the diameter of 20 mm in spacing of 150 mm),
- web of precast element: both sided #10/100.

In adopted approach (in the [3] called as approach C), reinforcement is considered in every stress state, no matter whether it is compressed or tensioned. The hybrid beam is thus modelled as a structure consisting of five materials: one steel and four types of homogenised RC (*in-situ* slab, upper slab of precast element, web of precast element, bottom slab of precast element – all of these with different concrete class and/or reinforcement ratio). Appropriate stress–strain curves are assigned for the entire regions with the same concrete thickness, concrete class and reinforcement ratio. Geometry of the beam is presented in Fig. 8.

Actions applied to the girder were taken directly from a real bridge analysis as:

- self-weight of the precast element + *in-situ* slab (density of concrete 25 kN/m³, of steel 78.5 kN/m³);
- self-weight of surface layers – as uniformly distributed with a value of 2.65 kPa;
- uniformly distributed load (UDL) – 9 kPa, applied to the first, second or both spans and
- tandem system (TS) load – 2×300 kN moving along the entire girder.

These loads allowed to obtain bending moments in a girder that are very close to moments in a real bridge, thus real cracking conditions are expected. The FE model was made in e^2p^3 class [24] with all elements modelized with shell elements, as shown in Fig. 9.
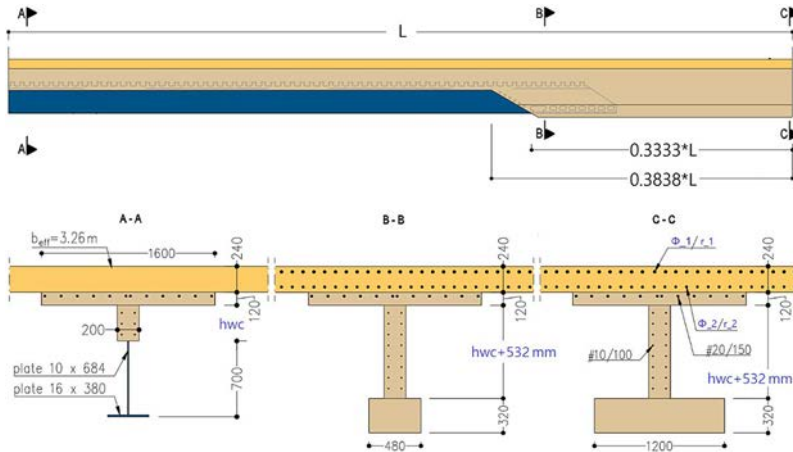
Fig. 8. Hybrid beam assumed for FE analysis (rebars only in the tensile regions are displayed)
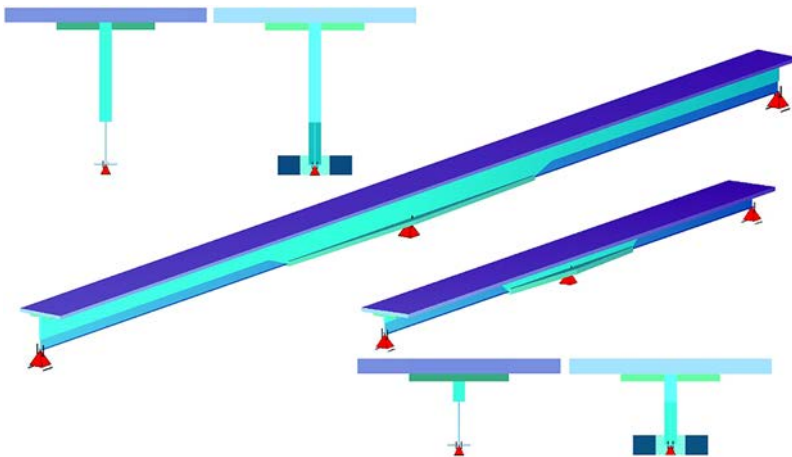
Fig. 9. 3D view and cross sections of a finite element model of the considered beams – 40 (upper-left) and 20 m (lower-right) span lengths (structural steel highlighted in blue, prefabricated concrete in cyan, and in-situ concrete in violet)

2.2. Tension stiffening effect

Analyses conducted in this article are based on the *approach C* coherently described and validated in the [3]. Hereafter the brief introduction to this approach is presented.

The following law for concrete elements was adopted (with distinction to elements with different reinforcement layouts). RC parts were modelled using a homogenised material that enables considering of tension stiffening effect for reinforcement and tension softening of the concrete by applying one stress–strain curve for each part of the RC members. This model is based on the stress–strain and force–strain relationships presented in [25–27].

These relationships were originally defined for embedded reinforcing steel, but the authors adopted them to concrete parts.

This approach of modelling of cracked reinforced parts is not strict and has some apparent inconsistencies. Firstly, longitudinal reinforcement may not be oriented in the same direction as principial stresses in the concrete. Tension stiffening effect is calculated on the basis of longitudinal reinfocement, but appears in finite element model in the direction of principal stresses. Moreover, when crack appears, Poisson's coefficient in the concrete could be reduced to 0 value, which also would affect the stiffness matrix in a two-dimensional shell finite element. Despite the abovementioned doubts presented in Fig. 10, the model law for concrete materials was adopted in performed analysis as a sufficient and relatively easy method in implementation. The validation of this method comparing to different possible approaches which are based on the Eurocode 4 [23] procedures is presented in the [3]. It was prooved that the convergence of obtained results is very high and adopted approach can be treated as justified.
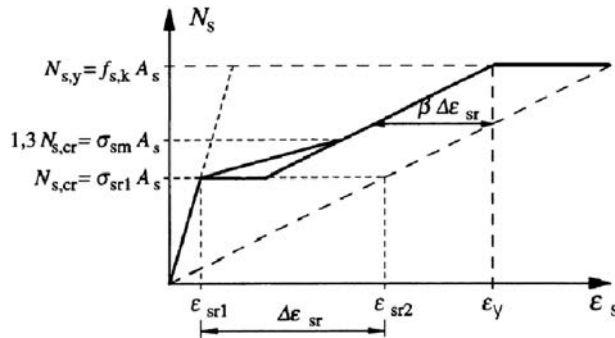
Fig. 10. Tension stiffening model adopted in analysis, according to annex L1 [25]

Application of the presented numerical method may be used to other construction members, for example columns. Automatic reduction of the reinforced concrete stiffeness due to its cracking may be used for calculation of curvature changes for the assesment of second order effects. The results may be compared with existing outcomes, e.g. [28].

2.3. Concrete rheology

Rheological parameters of shrinkage were calculated automatically via CSM (Construction Stage Manager) in SOFiSTiK [29]. Initial parameters were as following:
– Average temperature of concrete aging: $8°C$;
– Relative humidity of the ambient environment: 70%;
– Term of concrete care process: 7 days;
– Effective concrete age at the time of first external loading: 28 days.

It is important to notice that input parameters for calculation of creep and shrinkage values will of course affect somehow the final results, but are of minor importance for final conclusions presented hereafter.

2.4. Analysis workflow

Calculations were conducted according to the following steps.

2.4.1. Geometry of cross-sections

Firstly, theoretical span length was assumed (20, 25, 30, 35 and 40 m). All of the dimensions (except height of the concrete web – hwc in Fig. 8) of the cross sections were fixed. Height of the concrete web was determined for every span length. It was assumed that normal stresses (caused by characteristic values of variable and permenent loads) in the bottom flange in the span should be equal approximately to 260 MPa (what for ULS analysis of road bridges would give approx. $260 \cdot 1.35 = 351$ MPa, so the value close to yield strenght for S355 steel grade, or with some safety margin, for accounting also different loads like thermal and wind actions, settlements, etc. if S460 is adopted). The stresses were calculated using linear analysis and omitting rheological effects. To fullfil this condition corresponding height of the web was determinated iteratively (resluts in Table 1).

Table 1. Iteratively found hwc (height of concrete web) for particular girders' lengths

L	hwc
[m]	[m]
20	0.33
25	0.63
30	0.93
35	1.18
40	1.48

2.4.2. Predesign of reinforcement ratio

Knowing the proper geometry, stresses were integrated (via module SIR – Sectional Results in SOFiSTiK) over the intermediate support cross section to calculate hogging bending moment. To show how rheology and cracking affects redistribution of bending moments, it was assumed that results should cover realistic/applicable range of stresses in reinforcement. Two separate cases were analysed: first for 160 MPa in upper layer of reinforcement and second – 320 MPa in this layer. Stresses smaller than 160 MPa are treated as uneconomic, and highter than 320 MPa are found as nearly impossible to justified due to crack width limitation requirements in real bridge design. Therefore, using classical beam theory, stresses in upper and bottom layer of reinforcement was determined. The diameter of the reinforcement in the upper layer was assumed as:
   – in the case when 320 MPa was expected: $\Phi_1 = 25$ mm in the upper layer and $\Phi_2 = 20$ mm in the bottom layer,
   – in the case when 160 MPa was expected: $\Phi_1 = 32$ mm in the upper layer and $\Phi_2 = 25$ mm in the bottom layer.

The parameters which were changed in every particular case were rebar spacings – see r_1 and r_2 in Fig. 8 and Table 2.

Table 2. Parameters that describes geometry (L – length) and reinforcement (Φ_1, Φ_2, r_1, r_2 – diameter and spacing of rebars in upper and bottom layer) of analysed girders

L	160 MPa in the upper layer expected							320 MPa in the upper layer expected						
L	Φ_1	r_1	Φ_2	r_2	σ_B	σ_U	A	Φ_1	r_1	Φ_2	r_2	σ_B	σ_U	A
[m]			[mm]			[MPa]	[cm^2/m]			[mm]			[MPa]	[cm^2/m]
20	32	133	25	133	137	161	97	25	180	20	180	277	318	45
25	32	110	25	110	141	162	118	25	150	20	150	290	324	54
30	32	90	25	90	137	155	144	25	125	20	125	290	320	64
35	32	80	25	80	138	155	162	25	110	20	110	291	319	73
40	32	75	25	75	146	161	172	25	100	20	100	300	325	81

Rebar spacing assumed in other parts of construction (prefabricated slab/flange, concrete web and bottom flange) was the same in every case (see Fig. 8).

2.4.3. Stress-strain curves

Proper stress-strain curves were evaluated according to the Fig. 10 and assigned to the corresponding parts of the Finite Element model. Exemplary curve is shown in Fig. 11.
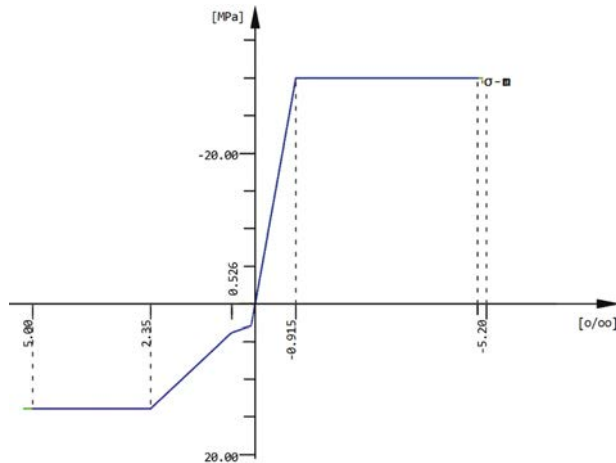
Fig. 11. Exemplary strain-stress curve for *in-situ* slab for $L = 40$ m and designed value of stress in rebar equals to 320 MPa

2.4.4. Live and non-rheological permanent loads

In order to obtain results that take into account tension stiffening effect a materially nonlinear analysis was conducted. In case of variable and permenent (dead) loads acting simultanously, the level of utilisation in RC parts results in exceeding tensile strength of the concrete. And thereby concrete cracking and tension-stiffenening effect may be visible and adequately captured.

2.4.5. Cracked zones – impact of level of load

In case when only permanent (and rheological) loads acting, by contrast, the level of utilisation is not that significant. Therefore cracking of concrete and tension-stiffenening effect would have been underestimated (in reality all abovementioned types of actions may interact). To bypass this issue, firstly linear analysis of the permanent (and rheological) loads (factor 1.00) was performed, and then, an auxiliary multiplication factor (*facd*) was calculated. The factor was evaluated as support bending moment M_{G+L} caused by variable and permanent (without rhelogy) loads divided by support bending moment M_{GPC} caused only by permanent (and rheological) loads, see Table 3.

Table 3. Support bending moments caused by different types of actions

L	M_{G+L}	M_{GPC}	*facd*
[m]	[kNm]	[kNm]	[–]
20	6 832	2 856	2.39
25	10 111	4 560	2.22
30	13 943	6 650	2.10
35	17 695	8 825	2.01
40	22 504	11 649	1.93

2.4.6. Rheological permanent loads

Then the subtantial analysis, where permanent (and rheological) loads was multiplicated by the above-described factor, was conducted. This allowed to properly reflect distribution of cracked zones and resulting tension-stiffening effect. Obtained this way bending moments are of course *facd*-times bigger than the real ones, so for the purposes of evaluating the changes in moments due to rheology, bending moments will be divided again by the *facd*-factor.

With the aim to separate influence of creep from influence of shrinkage and simultaneously take into account cracking, nonlinear analysis was performed twice. Firstly assuming that creep and shrinkage can evolve together, secondly assuming absence of effects of shrinkage.

3. Results

To obtain readable results, internal moments were calculated from the stress state via an integration (via SIR module in SOFiSTiK [29]) at the intersection at every one-tenth of the span length. Below it is presented how bending moments has changed due to concrete cracking (columns marked as N-160 and N-320 describe nonlinear analysis allowing for concrete cracking with 160 MPa or 320 MPa stress state in upper in-situ slab reinforcement, respectively) in comparison to uncracked analysis (described as Linear).

All results are presented in Table 4 to 11, among which Tables 4 and 5 show influence of concrete cracking on changes of maximum support and mid-span bending moments, respectively, Tables 6 to 9 show influence of concrete rheology, and finally Tables 10 to 11 show resultant changes in bending moments in comparison to base state (uncracked linear analysis without concrete rheology).

Table 4. Influence of reinforcement and type of conducted analysis on support bending moments

Maximal support moments					
L	Absolute values [kN·m]			Normalized values [%]		
[m]	Linear	N-160	N-320	Linear	N-160	N-320
20	–6 832	–6 328	–6 051	100.0	92.6	88.6
25	–10 111	–9 353	–8 855	100.0	92.5	87.6
30	–13 943	–12 987	–12 115	100.0	93.1	86.9
35	–17 695	–16 794	–15 621	100.0	94.9	88.3
40	–22 504	–21 599	–20 064	100.0	96.0	89.2

Table 5. Influence of reinforcement and type of conducted analysis on mid-span bending moments

Maximal span moments					
L	Absolute values [kN·m]			Normalized values [%]		
[m]	Linear	N-160	N-320	Linear	N-160	N-320
20	3 702	3 810	3 869	100.0	102.9	104.5
25	5 274	5 440	5 589	100.0	103.1	106.0
30	7 193	7 347	7 608	100.0	102.1	105.8
35	9 322	9 491	9 875	100.0	101.8	105.9
40	11 799	11 997	12 505	100.0	101.7	106.0

Table 6. Influence of reinforcement and type of conducted analysis on support bending moments in dependence of considered rheological effects

Maximal support moments					
L	Absolute values [kN·m]			Normalized values [%]		
[m]	Linear	N-160	N-320	Linear	N-160	N-320
0 days						
20	–2 856	–2 645	–2 528	100.0	92.6	88.5
25	–4 560	–4 210	–3 974	100.0	92.3	87.1
30	–6 650	–6 163	–5 740	100.0	92.7	86.3

Continued on next page

Table 6 – *Continued from previous page*

L	Absolute values [kN·m]			Normalized values [%]		
	Maximal support moments					
[m]	Linear	N-160	N-320	Linear	N-160	N-320
35	–8 825	–8 335	–7 733	100.0	94.4	87.6
40	–11 649	–11 114	–10 298	100.0	95.4	88.4
	Creep – 100 years					
20	–2 350	–2 241	–2 181	100.0	95.3	92.8
25	–3 787	–3 590	–3 467	100.0	94.8	91.6
30	–5 614	–5 294	–5 098	100.0	94.3	90.8
35	–7 874	–7 463	–7 179	100.0	94.8	91.2
40	–10 585	–10 045	–9 669	100.0	94.9	91.3
	Creep & Shrinkage – 100 years					
20	–3 233	–3 028	–2 884	100.0	93.6	89.2
25	–4 904	–4 613	–4 377	100.0	94.1	89.3
30	–6 964	–6 575	–6 226	100.0	94.4	89.4
35	–9 413	–8 968	–8 518	100.0	95.3	90.5
40	–12 350	–11 797	–11 233	100.0	95.5	91.0
	Shrinkage – 100 years					
20	–883	–787	–703	100.0	89.1	79.6
25	–1 117	–1 024	–910	100.0	91.6	81.5
30	–1 350	–1 281	–1 128	100.0	94.9	83.5
35	–1 539	–1 505	–1 339	100.0	97.8	87.0
40	–1 765	–1 752	–1 565	100.0	99.3	88.7

Table 7. Influence of reinforcement and type of conducted analysis on span bending moments
in dependence of considered rheological effects

L	Absolute values [kN·m]			Normalized values [%]		
	Maximal span moments					
[m]	Linear	N-160	N-320	Linear	N-160	N-320
	0 days					
20	728	799	839	100.0	109.9	115.3
25	1 204	1 320	1 406	100.0	109.6	116.7
30	1 813	1 992	2 136	100.0	109.9	117.8
35	2 639	2 818	3 033	100.0	106.8	114.9
40	3 654	3 845	4 132	100.0	105.2	113.1

Table 7 – *Continued from previous page*

L	Absolute values [kN·m]			Normalized values [%]		
Maximal span moments						
[m]	Linear	N-160	N-320	Linear	N-160	N-320
Creep – 100 years						
20	875	921	947	100.0	105.3	108.2
25	1 438	1 522	1 575	100.0	105.8	109.5
30	2 166	2 292	2 377	100.0	105.8	109.8
35	3 059	3 238	3 360	100.0	105.9	109.8
40	4 151	4 398	4 558	100.0	106.0	109.8
Creep & Shrinkage – 100 years						
20	612	674	720	100.0	110.1	117.7
25	1 093	1 180	1 256	100.0	108.0	115.0
30	1 723	1 854	1 961	100.0	107.6	113.8
35	2 577	2 721	2 864	100.0	105.6	111.1
40	3 612	3 791	3 968	100.0	105.0	109.9

Table 8. Influence of reinforcement and type of conducted analysis on support bending moments in dependence of the stage of life of construction

L	0 days			Creep & Shrinkage – 100 years		
Maximal support moments						
[m]	Linear	N-160	N-320	Linear	N-160	N-320
Absolute values [kN·m]						
20	–2 856	–2 645	–2 528	–3 233	–3 028	–2 884
25	–4 560	–4 210	–3 974	–4 904	–4 613	–4 377
30	–6 650	–6 163	–5 740	–6 964	–6 575	–6 226
35	–8 825	–8 335	–7 733	–9 413	–8 968	–8 518
40	–11 649	–11 114	–10 298	–12 350	–11 797	–11 233
Normalized values [%]						
20	100.0	92.6	88.5	113.2	106.0	101.0
25	100.0	92.3	87.1	107.5	101.2	96.0
30	100.0	92.7	86.3	104.7	98.9	93.6
35	100.0	94.4	87.6	106.7	101.6	96.5
40	100.0	95.4	88.4	106.0	101.3	96.4

Table 9. Influence of reinforcement and type of conducted analysis on span bending moments
in dependence of the stage of life of construction

Maximal span moments						
L	0 days			Creep & Shrinkage – 100 years		
[m]	Linear	N-160	N-320	Linear	N-160	N-320
Absolute values [kN·m]						
20	728	799	839	612	674	720
25	1 204	1 320	1 406	1 093	1 180	1 256
30	1 813	1 992	2 136	1 723	1 854	1 961
35	2 639	2 818	3 033	2 577	2 721	2 864
40	3 654	3 845	4 132	3 612	3 791	3 968
Normalized values [%]						
20	100.0	109.9	115.3	84.2	92.7	99.0
25	100.0	109.6	116.7	90.7	98.0	104.3
30	100.0	109.9	117.8	95.0	102.2	108.1
35	100.0	106.8	114.9	97.6	103.1	108.5
40	100.0	105.2	113.1	98.9	103.8	108.6

Table 10. Influence of reinforcement and type of conducted analysis on support bending moments
in dependence of the stage of life of construction (variable and permanent loads)

Maximal support moments						
L	0 days			after 100 years		
[m]	Linear	N-160	N-320	Linear	N-160	N-320
Absolute values [kN·m]						
20	–6 832	–6 328	–6 051	–7 209	–6 711	–6 406
25	–10 111	–9 353	–8 855	–10 455	–9 757	–9 259
30	–13 943	–12 987	–12 115	–14 258	–13 399	–12 601
35	–17 695	–16 794	–15 621	–18 283	–17 427	–16 406
40	–22 504	–21 599	–20 064	–23 205	–22 282	–20 999
Normalized values [%]						
20	100.0	92.6	88.6	105.5	98.2	93.8
25	100.0	92.5	87.6	103.4	96.5	91.6
30	100.0	93.1	86.9	102.3	96.1	90.4
35	100.0	94.9	88.3	103.3	98.5	92.7
40	100.0	96.0	89.2	103.1	99.0	93.3

Table 11. Influence of reinforcement and type of conducted analysis on span bending moments
in dependence of the stage of life of construction (variable and permanent loads)

Maximal span moments						
L	0 days			after 100 years		
[m]	Linear	N-160	N-320	Linear	N-160	N-320
	Absolute values [kN·m]					
20	3 702	3 810	3 869	3 587	3 685	3 751
25	5 274	5 440	5 589	5 163	5 300	5 440
30	7 193	7 347	7 608	7 102	7 208	7 432
35	9 322	9 491	9 875	9 259	9 394	9 705
40	11 799	11 997	12 505	11 757	11 943	12 340
	Normalized values [%]					
20	100.0	102.9	104.5	96.9	99.5	101.3
25	100.0	103.1	106.0	97.9	100.5	103.1
30	100.0	102.1	105.8	98.7	100.2	103.3
35	100.0	101.8	105.9	99.3	100.8	104.1
40	100.0	101.7	106.0	99.6	101.2	104.6

4. Discussion on results

On basis of performed analysis one can conclude as follows.

1. Tables 4 and 5. In case of variable loads and dead loads acting together (without rheological effects), when stresses in the upper reinforcement are assumed to be equal to 160 MPa, support moments are reduced by 4.0 to 7.5%. In the same way mid-span moments are increased accordingly, in considered case by 1.7 to 3.1%.

2. Tables 4 and 5. As above, but stresses in the upper reinforcement are assumed to be equal to 320 MPa, support moments are reduced by 10.8 to 13.1%, mid-span moments are increased by 4.5 to 6.0%.

3. Tables 6 and 7. In case of dead loads and creep acting together (without shrinkage), when stresses in the upper reinforcement are assumed to be equal to 160 MPa, support moments are reduced by 4.7 to 5.7%, mid-span moments are increased by 5.3 to 6.0%.

4. Tables 6 and 7. As above, but stresses in the upper reinforcement are assumed to be equal to 320 MPa, support moments are reduced by 7.2 to 9.2%, mid-span moments are increased by 8.2 to 9.8%.

5. Tables 6 and 7. In case of dead loads and rheology acting together (both creep and shrinkage), when stresses in the upper reinforcement are assumed to be equal to 160 MPa, support moments are reduced by 4.5 to 6.4%, mid-span moments are increased by 5.0 to 10.1%.

6. Tables 6 and 7. As above, but stresses in the upper reinforcement are assumed to be equal to 320 MPa, support moments are reduced by 9.0 to 10.8%, mid-span moments are increased by 9.9 to 17.7%.

Abovementioned results are calculated in regards to the linear analysis, in which rheological effects where incorporated. With the aim of simplifying design calculations, its more informative to compare results with so-called base state, where rheological and cracking effects are ommited.

7. Tables 8 and 9. In case of dead loads and rheology acting together (both creep and shrinkage), when stresses in the upper reinforcement are assumed to be equal to 160 MPa, support moments are reduced by 1.1% or even have to be amplified by 6.0%, mid-span moments are increased by up to 3.8%, but, in some cases, are reduced by up to 7.3%.

8. Tables 8 and 9. As above, but stresses in the upper reinforcement are assumed to be equal to 320 MPa, support moments are reduced by 6.4% or even have to be amplified by 1.0%, mid-span moments are increased by up to 8.6%, but, in some cases, are reduced by up to 1.0%.

Finally, comparison of effects of all loads (variable and permenent) for every construction age (envelope for $t = 0$ to $t = 100$ years) with so-called base state (linear analysis without concrete cracking and without consideration of concrete rheology) is presented.

9. Tables 10 and 11. In case of variable loads, dead loads and, alternatively, rheology acting together (both creep and shrinkage), when stresses in the upper reinforcement are assumed to be equal to 160 MPa, support moments are reduced by 1.0 to 7.5% and mid-span moments are increased by up to 3.1% (or even may be reduced in some cases by 0.5%).

10. Tables 10 and 11. In case of variable loads, dead loads and, alternatively, rheology acting together (both creep and shrinkage), when stresses in the upper reinforcement are assumed to be equal to 320 MPa, support moments are reduced by 6.2 to 13.1% and mid-span moments are increased by 1.3 to 6.0%.

It is essential to point out that results presented in this article were calculated for specific construction with particular ratios of variable to permanent loads. For example, impact of shrinkage varies on the magnitude of external loading. However, results for different ratios of variable to permanent loads could be easily calculated basing on given partial results, broadening the scope of presesented analyses.

5. Conclusions

Scale of the redistribution of bending moments, as can be concluded basing on all Tables 4 to 11, strongly depends on the reinforcement ratio in the hybrid beam parts under tension. Comparing uncracked state without rheology (with both variable and perment loads) with nonlinear analysis covering cracking and rheology for both $t = 0$ and $t = 100$ years, it may be deduced that – depending on the stresses in the bars – support moments are reduced in performed analysis by 1.0 to 13.1% and mid-span moments are increased, accordingly, by –0.5 to 6.0%.

As a design rule for performing global analysis of hybrid beams authors propose a design approach completly reversed to the concept used as standard in EC4 [23]: uncracked analysis, and at the stage of postprocessing to perform appropriate bending moment redistribution. If concrete rheology is not considered in FE model, bending moments redistribution limits could be estimated safe-sided as follow:

– for assessment of hogging bending moments (in zones of intermediate supports):
  - if stresses in upper in-situ slab reinforcement are 160 MPa: no reduction of hogging moments (in reality a reduction of $1 - 4\%$ can be expected after 100 years),
  - if stresses in upper in-situ slab reinforcement are 320 MPa: 5% reduction of hogging moments (in reality a reduction of 6–10% can be expected after 100 years);
– for assessment of sagging bending moments (in mid-span zones):
  - if stresses in upper in-situ slab reinforcement are 160 MPa: 10% reduction of hogging moments (in reality a reduction of 4–8% can be expected at $t = 0$ right after concrete cracking) and appropriate increase in sagging moments at mid-span,
  - if stresses in upper in-situ slab reinforcement are 320 MPa: 15% reduction of hogging moments (in reality a reduction of 11–13% can be expected at $t = 0$ right after concrete cracking) and appropriate increase in sagging moments at mid-span.

For stresses in upper reinforcement between 160 and 320 MPa intermadiate values of bending moments redistribution can be adopted. The presented concept of global elastic analysis enables easy modelling of hybrid beams (uncracked sections, alternatively no rheology considered too) with safe-sided assumptions for both hogging and sagging moment regions. This approach is the result of a broader look at the experience gained during the design and construction of structures presented in [1, 3, 5, 6, 14, 21] and broaden by quantitative analysis described herein.

The proposal to use the analysis in the uncracked state in the analysis of hybrid beams is strongly justified, because apart from the fundamental quantitative issue of moment redistribution, demonstrated by the analyzes in this article, there are two important factors in favor of its introduction. Firstly, observation, that hybrid structures represents a new idea of reinforced concrete using rigid steel elements [30] strongly justifies the proposal from a historical and logical point of view of theory of concrete structures. Secondly, the departure from the modeling of the cracked concrete at the hogging bending zone of composite beams is a great technical simplification in the case of modern methods of modeling structures using FEM: it enables efficient concrete dimensioning with automatic modules in relation to the shell elements of the deck slab (as opposed to the controversial procedures that take into account cracking and the tension stiffening effect), while in the case of a midspan region only one result (bending moment or the appropriate normal stress) is multiplied by a factor. Thus, the new concept, which is de facto a reversal of the Eurocode 4 procedure, is justified on many levels and it results not from the desire to change the existing rules, but from the desire to systematically solve the difficulties that the authors encountered when designing hybrid beams in accordance with the applicable procedures. Currently, a contract is being implemented, where many hybrid objects with a geometry similar to the one described in the article are being built: test loads of these objects and evaluation of their behavior will allow for a thorough verification of the proposed concept in practice.

References

[1] W. Lorenc, "Composite dowels: the way to the new forms of steel-concrete composite structures", *Synergy of Culture and Civil Engineering – History and Challenges – IABSE Symposium 7-9 October 2020, Wrocław, Poland*. IABSE, 2020, pp. 98–138, doi: 10.2749/wroclaw.2020.0093.

[2] W. Lorenc and B. Bartoszek, "The new railway hybrid bridge in Dąbrowa Górnicza: innovative concept using new design method and results of load tests", *Studia Geotechnica et Mechanica,* vol. 45, no. 2, pp. 89–111, 2023, doi: 10.2478/sgem-2023-0002.

[3] M. Kożuch and Ł. Skrętkowicz, "Proposal of concept for structural modelling of hybrid beams", *Studia Geotechnica et Mechanica*, vol. 44, no. 4, pp. 317–332, 2022, doi: 10.2478/sgem-2022-0023.

[4] W. Lorenc and G. Seidl, "Composite dowels for bridges: trends and challenges for new European design rules", presented at 9th International conference on composite construction in steel and concrete, 27-29 July 2021, online, Germany, 2021.

[5] W. Kosecki, T. Kołakowski, R. Lewandowski, K. Bartosz, K. Sumińska, M. Lipski, M. Kożuch, P. Kozioł, W. Lorenc, and K. Marcinczak, "Nowe belki hybrydowe w obiektach mostowych na drodze ekspresowej S3 Troszyn–Świnoujście", presented at Seminarium Naukowo-Techniczne Wrocławskie Dni Mostowe, 24-25 November 2022, Wrocław, Poland, 2022.

[6] M. Kożuch, W. Lorenc, B. Bartoszek, A. Stempniewicz, H. Windorpski, M. Struczyński, R. Sęk, and W. Ochojski, "Application of rolled sections in composite bridges with span over 50 m", presented at 9th International Conference on Composite Construction in Steel and Concrete, 27–29 July 2021, online, Germany, 2021.

[7] M. Kożuch, H. Windorpski, M. Struczyński, and W. Ochojski, "Mosty zespolone o konstrukcji Krokodyl o rozpiętości przęsła 50–60 m", presented at Seminarium Naukowo-Techniczne Wrocławskie Dni Mostowe, 24-25 November 2022, Wrocław, Poland, 2022.

[8] T. Kaczmarek, T. Galewski, K. Topolewicz, R. Sęk, A. Radziecki, W. Ochojski, M. Kożuch, and W. Lorenc, "Polish experience with network arch bridges using coldbent HD sections", *Steel Construction*, vol. 13, no. 4, pp. 271–279, 2020, doi: 10.1002/stco.202000034.

[9] G. Seidl, E. Viefhues, J. Berthellemy, I. Mangerig, R. Wagner, W. Lorenc, M. Kożuch, J.M. Franssen, D. Janssen, J. Ikäheimonen, R. Lundmark, O. Hechler, and N. Popa, *RFCS research project PrEco-Beam: Prefabricated enduring composite beams based on innovative shear transmission. EUR 25321 EN*. Brussels: European Commission, 2013.

[10] M. Feldmann, F. Möller, S. Möller, P. Collin, R. Hällmark, O. Kerokoski, W. Lorenc, M. Kożuch, S. Rowiński, M. Nilsson, L. Astrom, B. Norlin, G. Seidl, T. Hehne, O. Hoyer, M. Stambuk, and T. Hariu, *ELEM: Composite bridges with prefabricated decks. EUR 25897 EN*. Brussels: European Commission, 2013.

[11] G. Seidl, N. Popa, R. Zanon, W. Lorenc, M. Kożuch, S. Rowiński, J.-M. Franssen, T. Fohn, C. Hermosilla, A. Farhang, and G. Nüsse, *RFCS dissemination knowledge project PRECO+: Prefabricated Enduring Composite Beams based on Innovative Shear Transmission. EUR 27834 EN*. Brussels: European Commission, 2014.

[12] W. Lorenc, T. Kołakowski, A. Hukowicz, and G. Seidl, "Verbundbrücke bei Elbląg Weiterentwicklung der VFT-WIB-Bauweise", *Stahlbau*, vol. 86, no. 2, pp. 167–174, 2017, doi: 10.1002/stab.201710463.

[13] W. Lorenc and G. Seidl, "Innovative Konstruktionen im Verbundbrückenbau mit Verbunddübelleisten", *Stahlbau*, vol. 87, no. 6, pp. 547–554, 2018, doi: 10.1002/stab.201810617.

[14] B. Bartoszek, A. Stempniewicz, W. Ochojski, A. Adamczyk, G. Natonek, and W. Lorenc, "Railway bridge in Dąbrowa Górnicza using composite dowels: new system development of composite railway bridges (Most kolejowy w Dąbrowie Górniczej z zastosowaniem zespolenia composite dowels: opracowanie nowego system zespolonych mostów kolejowych)", presented at WDM Symposium 2019, Wrocław, Poland, 2019.

[15] W. Lorenc, A. Stempniewicz, and B. Bartoszek, *New kind of externally reinforced structure of railway bridge with low construction height using rolled sections and composite dowels. R&D Final Report (Internal report for ArcelorMittal company*, 2019.

[16] R. Johnson, "Vertical shear in hybrid composite cross-sections of beams", presented at WDM Symposium 2021, Wrocław, Poland, 2021.

[17] W. Lorenc, "Przenoszenie siły poprzecznej a definicja konstrukcji zespolonej", *Mosty*, no. 6, 2011.

[18] W. Lorenc, "The model for a general composite section resulting from the introduction of composite dowels", *Steel Construction*, vol. 10, no. 2, pp. 154–167, 2017, doi: 10.1002/stco.201710019.

[19] W. Lorenc, S. Balcerowiak, J. Czajkowski, and J. Dobrzański, "The coherent concept of the lever arm in a cross-section", presented at IABSE Symposium 2020, Wrocław, Poland, doi: 10.2749/wroclaw.2020.0684.

[20] M. Kożuch, "Belki hybrydowe w mostach: definicja i koncepcja projektowania", *Mosty*, no. 4, pp. 40–42, 2021.

[21] W. Lorenc and M. Kożuch, "Introduction to hybrid sections and hybrid beams in bridges", presented at WDM Symposium 2021, Wrocław, Poland, 2021.

[22] EN 1992 Eurocode 2: Design of concrete structures (all parts).

[23] EN 1994 Eurocode 4: Design of composite steel and concrete structures (all parts).

[24] J. Bień, "Modelling of structure geometry in Bridge Management Systems", *Archives of Civil and Mechanical Engineering*, vol. 11, no. 3, pp. 519–532, 2011, doi: 10.1016/S1644-9665(12)60099-5.

[25] ENV 1994-2: 2001 Eurocode 4: Design of composite steel and concrete structures, Part 2: composite bridges.

[26] C. Hendry and P. Johnson, *Designers' guide to EN 1994-2 Eurocode 4: Design of steel and composite structures*. Thomas Telford, 2006.

[27] CEP-FIB Model Code 2010.

[28] J. Pędziwiatr and M. Musiał, "Calculation of second-order effects in columns – applications and examples", *Archives of Civil Engineering*, vol. 69, no. 1, pp. 271–286, 2023, doi: 10.24425/ace.2023.144173.

[29] SOFiSTiK, *ASE (General Static Analysis of Finite Element Structures) Manual*. Oberschleißheim, Germany: SOFiSTiK, 2020.

[30] W. Lorenc and J. Biliszczuk, "Konstrukcje hybrydowe – nowa idea żelbetu zbrojonego sztywnymi elementami stalowymi", (Hybrid structures – a new idea of reinforced concrete using rigid steel elements), presented at 11 Konferencja Dni Betonu, Wisła, 2021.

Koncepcja globalnej analizy statycznej belek hybrydowych – analizy numeryczne

Słowa kluczowe: most zespolony, belka hybrydowa, efekt tension-stiffening, zespolenie composite dowels

Streszczenie:

W artykule przedstawiono rozważania związane z globalną analizą statyczną belek hybrydowych, czyli takich, w których występują przekroje hybrydowe. Przekrój hybrydowy złożony jest z części stalowej oraz betonowej, połączonych ze sobą zespoleniem typu *composite dowels*, w którym obie części (stalowa i betonowa) biorą niepomijalny udział w przenoszeniu ścinania poprzecznego (w przeciwieństwie do standardowych przekrojów zespolonych stalowo – betonowych, które składają się z belki stalowej i umieszczonej na niej płyty betonowej, pomijanej zazwyczaj w analizie ścinania poprzecznego). W praktyce stosuje się też (w mostach) rozwiązania bardziej ogólne, w których w strefach przęsłowych belek ciągłych wykorzystuje się przekroje hybrydowe, natomiast w strefach podporowych – przekroje betonowe. Przedstawiono przykłady takich obiektów. Opisywane rozwiązania są nowe i wymagają też nowego podejścia w procesie projektowania. Kwestia nośności (na zginanie, siłę osiową oraz ścinanie) samego przekroju poprzecznego została już opisana, brak jest jednak wytycznych co do prowadzenia globalnej analizy statycznej. Inaczej bowiem, niż w przypadku stosowanych do tej pory belek stalowych zespolonych z płytą betonową, zarysowanie części

betonowych ma miejsce nie tylko w samej płycie betonowej, ale też w betonowych środnikach przekrojów hybrydowych, i to zarówno w strefach momentów ujemnych, jak i dodatnich. Wpływa to na swoistą dla belek hybrydowych redystrybucję momentów zginających. Również reologia betonu ma inny wpływ na wzbudzane siły wewnętrzne niż w przypadku standardowych belek zespolonych. Zagadnienia wpływu zarysowania betonu oraz jego reologii na redystrybucję siłwewnętrznych w belkach hybrydowych są przedmiotem niniejszego artykułu. Przedstawiono sposób modelowania efektu *tension-stiffening* z wykorzystaniem materiałowo nieliniowej analizy. Zbadano wpływ zarysowania betonu na siły wewnętrzne w belce w zależności od ilości zbrojenia w rozciąganych częściach betonowych. Obliczenia przeprowadzono dla czterech rozpiętości przęseł, od 10 do 40 m długości, przy założeniu schematu dwuprzęsłowej belki ciągłej. Geometrię (przekroje poprzeczne) dobrano tak, aby w części stalowej uzyskiwać naprężenia charakterystyczne ok. 260 MPa, a w zbrojeniu w strefie rozciąganej około 160 lub 320 MPa (rozważono te dwa przypadki jako skrajne oszacowania wartości mogących występować w realnej konstrukcji). Pokazano skalę redystrybucji w przypadku oddziaływania obciążeń grawitacyjnych: stałych i zmiennych oraz reologicznych: pełzania i skurczu oraz ich współdziałania. Ukazano zmiany momentu podporowego i przęsłowego, a wnioski uogólniono tak, aby możliwe było uproszczone szacowanie redystrybucji momentów także w układach wieloprzęsłowych. Na koniec przedstawiono wnioski prowadzące do powstania koncepcji globalnej analizy belek hybrydowych, w której autorzy proponują zupełne odwrócenie zasad opisanych w EN 1994. Zamiast przeprowadzać analizę w stanie zarysowanym (bardzo pracochłonną dla belek hybrydowych, wymagającą podejścia iteracyjnego) autorzy proponują globalną analizę sprężystą wykonywać w stanie niezarysowanym, a otrzymane siły wewnętrzne odpowiednio redystrybuować. Za takim podejściem przemawiają dwa fakty. Po pierwsze, belki hybrydowe reprezentują nową ideę konstrukcji betonowych zbrojonych sztywnym zewnętrznym elementem stalowym i takie podejście jest logiczne z punktu widzenia teorii konstrukcji betonowych. Po drugie stanowi to ogromne uproszczenie, szczególnie biorąc pod uwagę nowe możliwości modelowania za pomocą MES obiektów mostowych z wykorzystaniem elementów powłokowych do (co najmniej) odwzorowania płyty pomostowej. Analiza wykonywana w stanie niezarysowanym umożliwia automatyczne wymiarowanie zbrojenia, co jest bardzo dyskusyjne w przypadku wprowadzania redukcji sztywności tej płyty z uwagi na zarysowanie i efekt *tension-stiffening*. Proponowane zmiany, będące odwróceniem zasad opisanych w EN 1994 (tworzonym głównie z myślą o modelowaniu wyłącznie elementów belkowych) wynikają nie z chęci podważania tych zasad, ale z chęci systematycznego rozwiązywania problemów, na które autorzy publikacji napotkali przy projektowaniu mostów hybrydowych i jednoczesnej chęci wykorzystania istniejących procedur projektowych.